Bistability without Hysteresis: Electrochemically Driven Coupled Substrate Cycles

Emilie Simonet, Christian Bourdillon, and Jean-François Hervagault*

Unité Associée no. 6022 du Centre National de la Recherche Scientifique, Université de Compiègne, B.P. 20529, 60205 Compiègne Cedex 05, France

Received: June 23, 1998; In Final Form: October 9, 1998

The dynamic and steady-state behaviors of three coupled substrate cycles sharing interconversion enzymes are investigated in a homogeneous flow-through reactor (CSTR). Lactate dehydrogenase (LDH) converts pyruvate (Prv) and NADH into lactate (Lac) and NAD, respectively. In turn, NAD [and glucose 6-phosphate (Glc6*P*)] is recycled into NADH (and gluconolactone 6-phosphate) by glucose 6-phosphate dehydrogenase, and in the presence of ferricyanide (Ferri), Lac is reoxidized into Prv [and ferrocyanide (Ferro)]. Finally, Ferro is reoxidized in turn by a reticulated vitreous carbon (RVC) electrode poised at a controlled potential in a three-electrode configuration. Under thermodynamically open conditions with a constant supply of Prv, Ferri, NADH, and Glc6*P*, this multienzyme system exhibits irreversible transitions between alternative stable steady states (bistability without hysteresis) when the electrochemical rate of ferrocyanide recycling is varied. This nonlinear behavior results from the strong inhibition of LDH exerted by its substrate Prv. In the absence of an electrochemically driven recycling of ferrocyanide, only reversible bistability (dynamic hysteresis) may be observed [Simonet et al. *J. Phys. Chem.* **1996**, *100*, 19148]. The numerical predictions of a simple mathematical model taking into account the coupling between the actual enzyme rate equations, mass transfers, and electrochemical recycling agree both qualitatively and quantitatively with the observed experiments.

Introduction

The coexistence between two stable steady states, referred to as bistability, has long been known to occur far from equilibrium in (bio)chemical systems governed by appropriate nonlinear kinetic laws.[1] It is generally associated with the phenomenon of hysteresis in which a system jumps back and forth between the two branches of stable states for different critical values of a control parameter, corresponding to two limit points. The phenomenon is illustrated by a large number of experimental and theoretical studies in chemical[2−7] and biochemical systems.[8−14]

Bistability can, however, occur in the absence of hysteresis. Theoretical studies of biochemical reaction systems have shown that one of the limit points bounding the domain of bistability may not be accessible to the system. In such cases, the system can jump from one branch of (stable) steady states to the other but cannot undergo the reverse transition when the control parameter is varied across the bistability domain. The transition is therefore said to be irreversible.[15−25] Moreover, the analysis of the conditions under which bistability occurs in the absence of hysteresis in simple theoretical models for chemical systems based on fully reversible kinetic has demonstrated that the phenomenon is not an artifact produced by approximations in the derivation of the evolution equations.[26]

In the present communication we consider the dynamic and steady-state behaviors of a multienzyme system arranged in three coupled substrate cycles and operating under thermodynamically open conditions by in- and outfluxes of substrate and products (CSTR). We propose experimental evidence for the occurrence of irreversible transitions between alternative stable steady-state concentrations of the various metabolites.

Experimental Section

The experimental enzyme system under study is depicted and described in Figure 1. The evolution of the various metabolite concentrations is described by a set of three differential equations set to zero at steady state, and taking into account the actual reaction rates as determined under our experimental conditions, and fluxes throughout the reactor,[27] i.e.,

$$\frac{d[Prv]}{dt} = -\nu_{LDH} + \nu_{FCytb2} + \alpha([Prv]_0 - [Prv])$$

$$\frac{d[NADH]}{dt} = -\nu_{LDH} - \nu_i + \nu_{FDH} + \alpha([NADH]_0 - [NADH])$$

$$\frac{d[Ferri]}{dt} = \nu_e - 2\nu_{FCytb2} - \nu_i + \alpha([Ferri]_0 - [Ferri])$$

where α stands for the residence time within the reactor [=(in and out) flow rates/volume] and the subscript 0 refers to the influx concentrations. Prv is pyruvate, FCytb2 is flavocytochrome b2, LDH is lactate dehydrogenase, and Ferri is ferricyanide. The expressions of the various rate equations are given in the Appendix.

Provided that there is no influx of lactate (Lac), NAD and ferrocyanide (ferro) within the reactor, the equation system is complemented with the following mass conservation equations:

* Corresponding author. Present address: Unité de Recherche Associée no. 2227 du Centre National de la Recherche Scientifique, Bât. 440, Université de Paris-Sud, 91405 Orsay Cedex, France. E-mail: jean-francois.hervagault@ibaic.u-psud.fr.

10.1021/jp982725j CCC: $18.00
Published on Web 02/02/1999

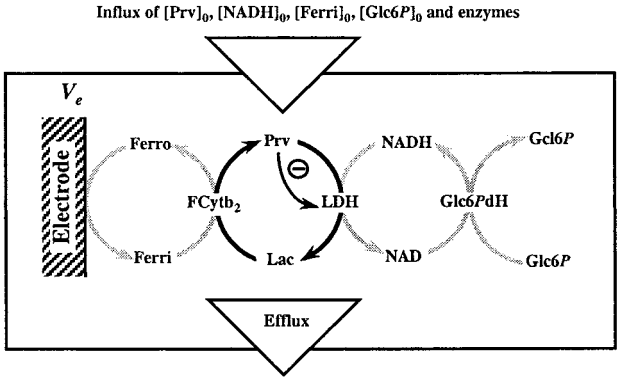

Figure 1. All reactions take place in a flow-through reaction chamber (CSTR) maintained at constant temperature (25 °C) and volume (3 mL), with equal in- and outflux rates (30 μL min^{-1}). The inlet solution contains pyruvate (Prv), NADH, ferricyanide (Ferri), glucose 6-phosphate (Glc6*P*), and enzymes, i.e., lactic dehydrogenase (LDH), glucose 6-phosphate dehydrogenase (Glc6*P*dH), and flavocytochrome b_2 (FCytb$_2$). The outlet solution contains all metabolites and enzymes. Within the reaction chamber, Prv and NADH are oxidized to lactate (Lac) and NAD, respectively, by LDH. Prv inhibits its own degradation by LDH (substrate inhibition). In the presence of Glc6*P* at saturating concentration, NAD is reduced in turn by Glc6*P*dH, with the production of gluconolactone 6-phosphate (Gcl6*P*). Lac and Ferri are reoxidized and reduced into Prv and ferrocyanide (Ferro), respectively, by FCytb$_2$. Finally, Ferri is reoxidized in turn by a large-area working electrode made of reticulated vitreous carbon (RVC) and poised at a controlled potential in a three-electrode configuration.[31] The counter electrode is separated from the main compartment by a glass frit.

$$[\mathrm{Prv}]_0 = [\mathrm{Prv}] + [\mathrm{Lac}]$$

$$[\mathrm{NADH}]_0 = [\mathrm{NADH}] + [\mathrm{NAD}]$$

$$[\mathrm{Ferri}]_0 = [\mathrm{Ferri}] + [\mathrm{Ferro}]$$

In the absence of any recycling of ferricyanide (electrochemical rate $\nu_e = 0$), the system (or a similar one) exhibits reversible bistability (dynamic hysteresis) when using, among other possible candidates, the influx pyruvate concentration, [Prv]$_0$, as the control parameter.[27] The steady-state concentration of pyruvate, [Prv], and all other metabolites ([NADH] and [Ferri]), exhibit an S-shaped dependency with respect to [Prv]$_0$, where the two limit points on the abcissa take a positive value.

The introduction of an electrochemically driven recycling of ferricyanide allows us to control the thermodynamic state of the system, and by addition of an extra degree of freedom, it may reveal new and unexpected steady-state and dynamic properties. Although the coupling between an electrode and an enzyme reaction is largely made use of in the design of biosensors (e.g., enzyme electrodes), few studies deal with the introduction of an electrochemical reaction on the kinetic behavior of (bio)catalytic processes. Dynamic responses such as periodic, complex periodic, and chaotic resonances were observed after imposition of sinusoidal perturbations by an alternating electrical current on focal steady states close to a Hopf bifurcation point in the peroxidase−oxidase and in the Belousov−Zhabotinsky (BZ) reactions.[28] More related to our purpose, Dechert and Schneider[29] have shown that, by application of external electrical currents, the switching between bistable steady states and the shifting of monostable steady states of the BZ reaction could occur.

In our multienzyme system, ν_e, the electrochemical reoxidation rate of ferrocyanide can be experimentally controlled, i.e.,

$$\nu_e = \eta^*[\mathrm{Ferro}]$$

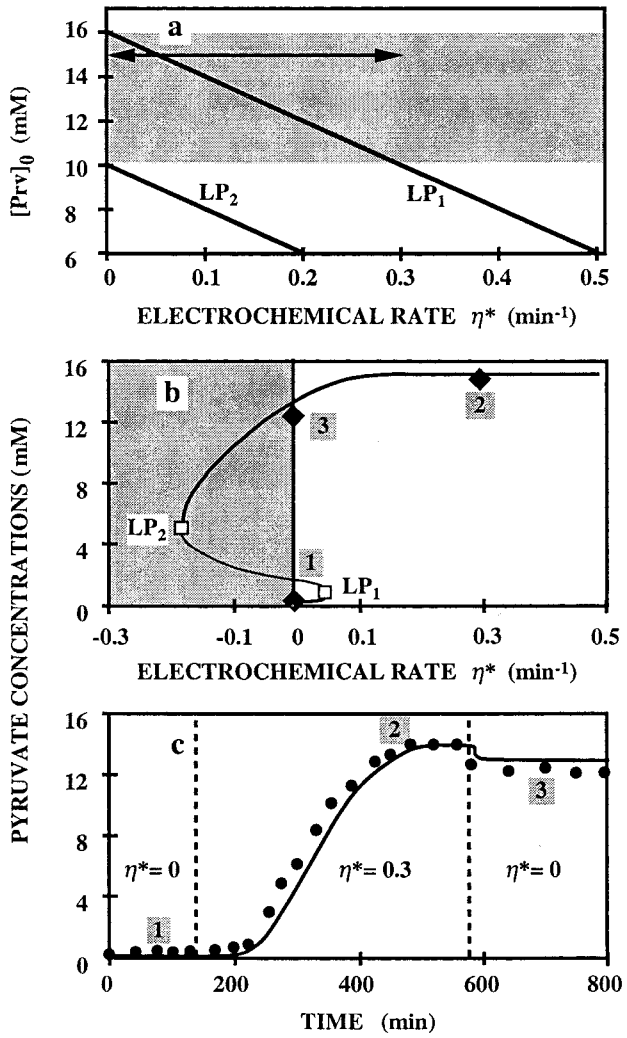

Figure 2. (a) Numerical continuation of limit points (LP$_1$ and LP$_2$) in the η^* parametric plane with $V_{M,LDH} = 0.25$ mM min^{-1}, $V_{M,Glc6PdH} = 0.4$ mM min^{-1}, $V_{M,Fcytb2} = 0.1$ mM min^{-1}, [ferri]$_0 = 0.5$ mM min^{-1}, [NADH]$_0 = 0.5$ mM, [Glc6*P*]$_0 = 40$ mM, and $\alpha = 0.01$ min^{-1} (residence time within the reactor). Irreversible transitions can be observed for [Prv]$_0$ comprised between 10 and 16 mM (gray area). The horizontal double arrow refers to the experimental conditions used in parts b and c with [Prv]$_0 = 15$ mM. All calculations were done by using the software package AUTO.[32] (b) Theoretical S-shaped dependency of the steady-state pyruvate concentration as a function of the electrochemical efficiency η^* for [Prv]$_0 = 15$ mM. Other parameters are as in part a. Labels 1−3 (and the associated black diamond symbols) refer to the experimentally observed steady states (see part c). Limit point LP$_2$ lies in the nonrealistic parameter domain (gray area). (c) Experimental observation of an irreversible transition under the parametric conditions as defined in parts a and b. The relaxation time between states 1 and 2 is about 5 h (3 times the residence time within the reactor), in agreement with the observations of Dechert and Schneider.[29] The curve through the experimental points was calculated from the equation set governing the system. The electrochemical rate commutes from 0 to 0.3 min^{-1} at $t = 150$ min and then from 0.3 back to 0 at $t = 530$ min (dotted lines).

where η^* is an apparent mass-transfer-controlled "rate constant" of the electrode reaction.[30] The continuation of the limit points in the [Prv]/η^* parametric plane (Figure 2a) shows that the phenomenon of multistability is (qualitatively) maintained and, more importantly, for a given range of [Prv]$_0$ (10−16 mM, under our experimental conditions), irreversible transitions can be observed when varying η^*. Figure 2b shows the steady-state pyruvate concentration ([Prv]) as a function of η^* for [Prv]$_0$ equal to 15 mM. Any point belonging to the resulting S-shaped

curve (including a limit point) with negative abcissa ($\eta^* < 0$) has no physical meaning in that it is not experimentally accessible. When the system is run under conditions where the initial [Prv] is close to zero [label 1 on the lower branch of steady-state solutions] and when η^* is increased from zero to a value greater than 0.05 min^{-1} (abcissa of LP_1), [Prv] will jump to the upper branch of stable steady states (label 2). By decreasing η^* down to zero, [Prv] will remain on that branch (label 3). In so far as the system cannot return to its initial situation (label 1), the transition (and unique possible one) between the two alternative steady states is of irreversible nature. The experimental demonstration of the phenomenon is shown in Figure 2c (see legend for details).

This direct and noninvasive perturbation method is actually able to drive the system from one steady-state solution to another. In other terms, the electrochemical reaction is able to entrain the whole enzyme system; in the experiment shown in Figure 2c, the intensity recorded on the electrode (for $\eta^* = 0.3$ min^{-1}) was around 0.92 mA, corresponding to an electrochemical flux ($J = i/nF$) equal to 9.5×10^{-9} mol s^{-1}, that is, $\nu_e = 0.126$ mM min^{-1}, which is a rate value of the same order of magnitude as those of the enzyme reactions occurring within the reactor.

Conclusion

Bistability without hysteresis probably has to be regarded as the most conspicuous and important property associated with multistationarity in that it might be involved in a variety of physical and physicochemical phenomena (e.g., ferromagnetic transitions, gas liquefaction, "pumping" in laser physics) and be of deep significance in view of its potential roles in differentiation and storage of information in a variety of biological contexts (e.g., immune system memory, long-term potentiation and/or depression during synaptic transmission, metabolic pathways, and cell cycle controls).

Appendix

L-Lactic dehydrogenase catalyses reversibly the reaction

$$\text{NADH} + \text{pyruvate} \leftrightarrow \text{NAD} + \text{lactate}$$

with an equilibrium constant equal to 1.8×10^{-6} at pH 7.

Under our experimental conditions, the enzyme operates irreversibly toward the right-hand side (oxidation and reduction of NADH and Prv, respectively). Indeed, further oxidation and reduction of the products Lac and NAD, respectively, proceed through irreversible steps.

It follows a sequential ordered mechanism with substrate inhibition by pyruvate:

$$\nu_{LDH} = \frac{V_{M,LDH}}{1 + \frac{K_{M,NADH}}{[NADH]} + \frac{K_{M,Prv}}{[Prv]} + \frac{K_{ia}K_{M,Prv}}{[NADH][Prv]} + \frac{[Prv]}{K_{i,Prv}}}$$

where $V_{M,LDH}$ is the maximal activity proportional to the enzyme concentration, $K_{M,NADH}$ and $K_{M,Prv}$ (13 and 29 mM, respectively) are the Michaelis constants for NADH and pyruvate, respectively, and $K_{i,Prv}$ (2 mM) is the inhibition constant for pyruvate. K_{ia} (83 μM) is a complex kinetic constant.

Flavocytochrome b2 oxidizes lactate (Lac) into pyruvate in the presence of ferricyanide (Ferri) and is inhibited noncompetitively by pyruvate:

$$\nu_{FCytb2} = \frac{V_{M,FCytb2}}{1 + \frac{K_{M,Lac}}{[Lac]} + \frac{K_{M,Ferri}}{[Ferri]} + \left(\frac{K_{M,Lac}K_{M,Ferri}}{[Lac][Ferri]}\right)\left(1 + \frac{[Prv]}{K_{i,Prv}}\right)}$$

where $V_{M,FCytb2}$ is the maximal activity for the enzyme and $K_{M,Lac}$ and $K_{M,Ferri}$ (0.25 mM and 13 μM, respectively) are the Michaelis constants for lactate and ferricyanide, respectively.

Formate dehydrogenase catalyses the reaction

$$\text{formate} + \text{NAD} \rightarrow \text{NADH} + CO_2$$

Under our experimental conditions, where the flux of N_2 through the reactor is enough to ensure a complete removal of the CO_2 produced by the reaction, this latter enzyme operates irreversibly toward the production of NADH. In addition, the enzyme is inhibited competitively by NADH. In the following rate expression, the concentration of formate is not taken explicitly into account, since its influx concentration is much larger than its Michaelis constant with respect to the enzyme:

$$\nu_{FDH} = \frac{V_{M,FDH}}{1 + \frac{K_{M,NAD}}{[NAD]} + \left(1 + \frac{[NADH]}{K_{i,NADH}}\right)}$$

where $V_{M,FDH}$ is the maximal activity of the enzyme and $K_{M,NAD}$ and $K_{i,NADH}$ (0.2 mM and 54 μM, respectively) are the Michaelis and inhibition constants for NAD and NADH, respectively.

Last, ν_i accounts for the nonenzymatic interactions between NADH and ferricyanide. This "interfering" reaction is first order with respect to both metabolites,

$$\nu_i = K_R[NADH][Ferri]$$

with $K_R = 18$ μM^{-1} min^{-1}, and the apparent electrochemical rate for the reoxidation of ferrocyanide, ν_e, can be defined as[30]

$$\nu_e = i/(nF\upsilon) = \eta^*[Ferro]$$

where i, n, F, and υ stand for the stationary current, the number of electrons exchanged (here, $n = 1$), the Faraday constant, and the reactor volume, respectively. The global first-order rate constant, η^* controlled by both the mass and electron transfers, takes nonexplicitly into account the electrode potential and rotation speed, the reticulated vitreous carbon (RVC) surface area, and the reactor geometry.

References and Notes

(1) Nicolis, G.; Prigogine, I. *Self-organization in non-equilibrium systems*; Wiley-Interscience: New York, 1977.
(2) Geiseler, W.; Föllner, H. H. *Biophys. Chem.* **1977**, *6*, 107.
(3) Schlögl, F. *Z. Physik* **1971**, *248*, 446.
(4) Schlögl, F. *Z. Physik* **1972**, *253*, 147.
(5) Orban, M.; Dateo, C.; De Kepper, P.; Epstein, I. R. *J. Am. Chem. Soc.* **1982**, *104*, 5911.
(6) Escher, C.; Ross, J. *J. Chem. Phys.* **1983**, *79*, 3773.
(7) Gray, P.; Scott, S. K. *Chemical oscillations and instabilities*; Clarendon Press: Oxford, 1994.
(8) Degn, H. *Nature* **1968**, *217*, 1047.
(9) Edelstein, B. B. *J. Theor. Biol.* **1970**, *29*, 57.
(10) Naparstek, A.; Romette, J. L.; Kernevez, J. P.; Thomas, D. *Nature* **1974**, *249*, 490.
(11) Eschrich, K.; Schellenberger, W.; Hofmann, E. *Eur. J. Biochem.* **1990**, *188*, 697.
(12) Laurent, M. *Biochem. J.* **1996**, *318*, 35.
(13) Kacser, H.; Small, J. R. *J. Theor. Biol.* **1996**, *182*, 209.
(14) Thomas, D.; Barbotin, J. N.; David, A.; Hervagault, J. F.; Romette, J. L. *Proc. Natl. Acad. Sci. U.S.A.* **1977**, *74*, 5314.
(15) Kaufman, M.; Andris, F.; Leo, O. *Int. Immunol.* **1996**, *8*, 613.

(16) Hahn, H. S.; Ortoleva, P.; Ross, J. *J. Theor. Biol.* **1973**, *41*, 503.
(17) Babloyantz, A.; Nicolis, G. *J. Theor. Biol.* **1972**, *34*, 185.
(18) Rapoport, T. A.; Heinrich, R. *Biosystems* **1975**, *7*, 120.
(19) Lisman, J. E. *Proc. Natl. Acad. Sci. U.S.A.* **1985**, *82*, 3055.
(20) Kaufman, M.; Thomas, R. *J. Theor. Biol.* **1987**, *129*, 141.
(21) Hervagault, J. F.; Canu, S. *J. Theor. Biol.* **1987**, *127*, 439.
(22) Hervagault, J. F.; Cimino, A. *J. Theor. Biol.* **1989**, *140*, 399.
(23) Hervagault, J. F.; Ortoleva, P.; Ross, J. *Proc. Natl. Acad. Sci. U.S.A.* **1991**, *88*, 10797.
(24) Hervagault, J. F.; Schellenberger, W. *J. Biol. Syst.* **1993**, *1*, 375.
(25) Fassy, F.; Renard, C.; Hervagault, J. F. *Biosystems* **1992**, *26*, 159.
(26) Guidi, G. M.; Goldbeter, A. *J. Phys. Chem. A* **1997**, *101*, 9367.
(27) Simonet, E.; Bourdillon, C.; Gervais, M.; Hervagault, J. F. *J. Phys. Chem.* **1996**, *100*, 19148.
(28) Förster, A.; Zeyer, K. P.; Schneider, F. W. *J. Phys. Chem.* **1995**, *99*, 11889.
(29) Dechert, G.; Schneider, F. W. *J. Phys. Chem.* **1994**, *98*, 3927.
(30) Bard, A. J.; Santhanam, K. S. V. In *Electroanalytical Chemistry*; Bard, A. J., Ed.; Marcel Dekker: New York, 1970; Vol. 4; pp 215−315.
(31) Laval, J. M.; Bourdillon, C.; Moiroux, J. *J. Am. Chem. Soc.* **1984**, *106*, 4701.
(32) Doedel, E. AUTO: a program for the automatic bifurcation analysis of autonomous systems. In *Tenth Manitoba Conference on Numerical Mathematics and Computation*; University of Manitoba: Winnipeg, 1981; pp 265−284.